

# Optical properties of Si-doped GaN

E. F. Schubert<sup>a)</sup>, I. D. Goepfert, and W. Grieshaber<sup>b)</sup>  
Center for Photonics Research and Department of Electrical and Computer Engineering,  
Boston University, Boston, Massachusetts 02215

J. M. Redwing  
ATMI, Danbury, Connecticut 06810

(Received 27 May 1997; accepted for publication 14 June 1997)

The optical properties of *n*-type GaN are investigated for Si doping concentrations ranging from  $5 \times 10^{16}$  to  $7 \times 10^{18} \text{ cm}^{-3}$ . The photoluminescence linewidth of the near-band gap optical transition increases from 47 to 78 meV as the doping concentration is increased. The broadening is modeled in terms of potential fluctuations caused by the random distribution of donor impurities. Good agreement is found between experimental and theoretical results. The intensity of the near-band-gap transition increases monotonically as the doping concentration is increased indicating that nonradiative transitions dominate at a low doping density. The comparison of absorption, luminescence, reflectance, and photorefectance measurements reveals the absence of a Stokes shift at room temperature demonstrating the intrinsic nature of the near-band edge transition. © 1997 American Institute of Physics. [S0003-6951(97)02033-0]

The optical properties of *n*-type GaN depend sensitively on the Si donor concentration. However, the dependence of deep-level transitions<sup>1-3</sup> and the overall radiative efficiency on the Si doping concentration have not been reported. Both an increase of the radiative efficiency<sup>4-6</sup> and a decrease in radiative efficiency<sup>5,6</sup> have been demonstrated for different dopants in GaAs and these trends are well understood. In this publication, the radiative efficiency and the linewidth of the near-band-gap optical transition in GaN are investigated. Furthermore, the radiative efficiency is measured as a function of the doping density.

The Si-doped GaN samples were grown by organometallic vapor phase epitaxy (OMVPE) on the *c*-plane of a sapphire substrate. The samples were grown at 1100 °C with a growth rate of 2 μm/h. The diluted silane (SiH<sub>4</sub>) doping precursor flux was systematically varied to achieve doping densities in the range of  $5 \times 10^{16}$ – $7 \times 10^{18} \text{ cm}^{-3}$ . The room temperature photoluminescence measurements were performed using a HeCd laser, emitting at 325 nm, with an excitation density of 3 W/cm<sup>2</sup>. The luminescence is dispersed in a 0.75 m spectrometer, detected by a GaAs photomultiplier and amplified using low-noise phase-sensitive ‘lock-in’ amplification.

The room-temperature photoluminescence spectrum of a Si-doped GaN sample is shown in Fig. 1. The spectrum displays an intense near-band edge transition which has been attributed to band-to-band recombination<sup>7</sup> as well as to excitonic recombination.<sup>7-10</sup> The strong intensity of the near-band edge transition is indicative of the high quality of the epitaxial films.

In addition to the near-band-gap transition, there is a weak transition centered at 2.2 eV which is commonly known as the yellow luminescence line.<sup>1-3</sup> This line has been proposed to be due to defects, with Ga vacancies<sup>11</sup> and iron impurities<sup>12</sup> being possible candidates. Recently, Grieshaber

*et al.*<sup>13</sup> reported a detailed study on yellow luminescence in GaN, in which the excitation density was varied over several orders of magnitude.

The inset of Fig. 1 shows the near-band edge transition of *n*-type GaN with different Si doping densities. Inspection of the spectra reveals that the linewidth of the transition increases from 47 to 77 meV as the doping concentration increases from  $5 \times 10^{16}$  to  $7 \times 10^{18} \text{ cm}^{-3}$ .

Next the luminescence line broadening is modeled in terms of potential fluctuations caused by the random distribution of doping impurities. Randomly distributed dopants lead to unavoidable fluctuations of the doping concentration on a microscopic scale. These microscopic concentration fluctuations result in potential fluctuations. Assuming that these potential fluctuations are sufficiently large, a noticeable broadening of luminescence lines will occur. To calculate the potential fluctuations, it is assumed that their effect is limited in distance to the screening radius, namely the Debye or the Thomas-Fermi screening radius for nondegenerate and degenerate doping concentrations, respectively.

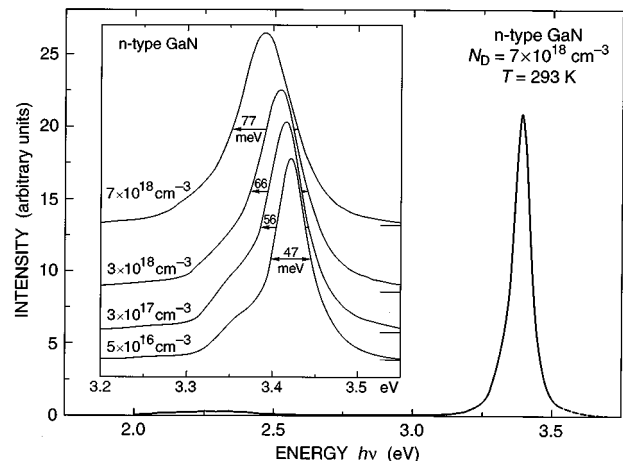


FIG. 1. Room temperature photoluminescence spectrum of *n*-type GaN at an excitation intensity of 3 W/cm<sup>2</sup>. The inset shows the near-band edge transition for *n*-type GaN doped at different Si concentrations.

<sup>a)</sup>Electronic mail: efs@bu.edu

<sup>b)</sup>Current address: Alcatel, Marcoussis, France.

The electronic donor and acceptor charge within the sphere defined by the screening radius is given by

$$Q = e(N_A + N_D)(4/3)\pi r_s^3, \quad (1)$$

where  $r_s$  is either the Debye or the Thomas–Fermi screening radius and  $e$  is the elementary charge. Assuming Poisson-distributed dopants, the mean charge fluctuation is given by

$$\Delta Q = \sqrt{e(N_A + N_D)(4/3)\pi r_s^3}. \quad (2)$$

From the charge fluctuation, the standard deviation of the potential fluctuation can be calculated. The potential at the location  $\mathbf{r}$  caused by a charge  $dQ$  located at  $\mathbf{r}_i$  is given by the screened Coulomb potential

$$d\Phi(\mathbf{r} - \mathbf{r}_i) = \frac{dQ}{4\pi\epsilon|\mathbf{r} - \mathbf{r}_i|} \exp\left(-\frac{|\mathbf{r} - \mathbf{r}_i|}{r_s}\right), \quad (3)$$

where  $\epsilon$  is the permittivity of GaN ( $\epsilon_r = 9.0$ ). Invoking the superposition principle, we obtain the total potential by integrating over all the differential charges, with the result

$$\Phi(\mathbf{r}) = \int_V \frac{dQ}{4\pi\epsilon|\mathbf{r} - \mathbf{r}_i|} \exp\left(-\frac{|\mathbf{r} - \mathbf{r}_i|}{r_s}\right). \quad (4)$$

The average potential deviation is then given by

$$\Delta\Phi = \frac{1}{V} \int_V \Phi(\mathbf{r}) dV, \quad (5)$$

where  $dV = 4\pi|\mathbf{r}|^2 d|\mathbf{r}|$ . This integral can only be evaluated numerically. In order to obtain an analytic expression, it is assumed that the entire fluctuating charge is located in the center of the sphere. The potential fluctuation at the average distance within the sphere, i.e., at  $r = (3/4)r_s$ , is then given by

$$\begin{aligned} \Delta\Phi &= \frac{e}{4\pi\epsilon} \frac{\sqrt{(N_D + N_A)} \frac{4}{3} \pi r_s^3}{(3/4)r_s} e^{-(3/4)(r_s/r_s)} \\ &= \frac{2e}{3\epsilon} \sqrt{(N_D + N_A)} \frac{r_s}{3\pi} e^{-3/4}. \end{aligned} \quad (6)$$

The broadening, i.e., full width at half-maximum (FWHM), of the near-band edge transition due to doping charge fluctuation is then given by

$$\Delta E_{\text{FWHM}} = \frac{2e^2}{3\pi\epsilon} \sqrt{(N_D + N_A)} \frac{\pi r_s}{3} e^{-(3/4)} 2\sqrt{2 \ln 2}, \quad (7)$$

where the factor  $2\sqrt{2 \ln 2}$  accounts for the difference between the standard deviation and the FWHM of a Gaussian distribution.<sup>14</sup>

The experimental and theoretical data are compared in Fig. 2. The FWHM given by Eq. (7) and the thermal broadening of the band-to-band transition, given by 1.8 kT, are shown in Fig. 2. In addition, the total broadening of the two uncorrelated broadening mechanisms is shown in Fig. 2. At low doping concentrations, the experimental linewidth is in agreement with thermal broadening. In the entire range of doping concentrations, the measured broadening is in excel-

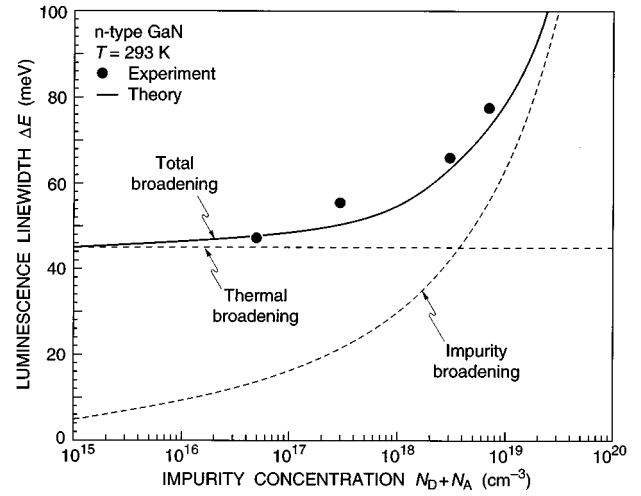


FIG. 2. Experimental linewidth of the near-band edge transition of *n*-type GaN as a function of the doping concentration. Also shown are the theoretical thermal broadening and broadening due to random impurity concentration fluctuations.

lent agreement with the calculated broadening due to potential fluctuations caused by the random distribution of dopants.

Note that band filling is not taken into account in the model presented here. Band filling effects do not play a role for  $n < N_c$ , where  $N_c$  is the effective density of states in GaN.<sup>15</sup> Band edge fluctuations due to the random distribution of impurities have also been calculated by Kane<sup>16</sup> and by Morgan.<sup>17</sup> The result of these authors also includes the  $\sqrt{(N_D + N_A)r_s}$  dependence of Eq. (7). However the numerical value for the line broadening obtained by Kane<sup>16</sup> and by Morgan<sup>17</sup> is two times larger than the value given by Eq. (7). Thus the agreement of the model presented here with experimental data is clearly better.

The intensity of the near-band edge transition increases markedly as the doping concentration increases. Figure 3 shows the peak intensity and the integrated intensity as a function of doping concentration. The integrated intensity increases by a factor of 6.5 as the doping density is increased from  $5 \times 10^{16}$  to  $7 \times 10^{18} \text{ cm}^{-3}$ . The relatively low intensity

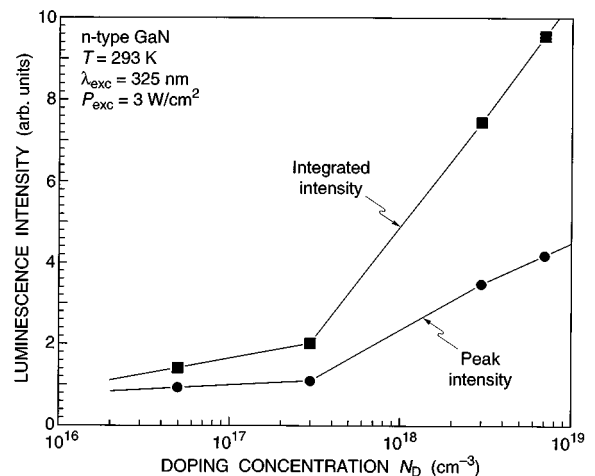


FIG. 3. Peak intensity and integrated intensity of the near-band edge transition of *n*-type GaN as a function of the doping concentration.

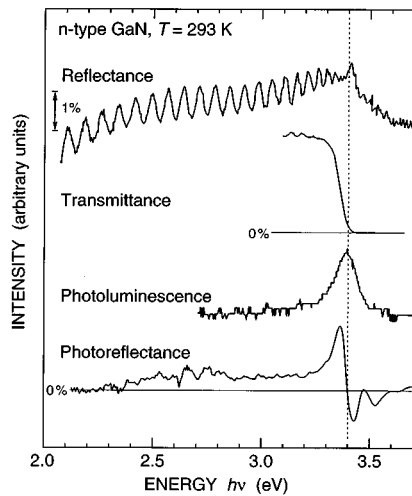


FIG. 4. Reflectance, transmittance, photoluminescence, and photoreflectance spectra of *n*-type GaN with a donor concentration of  $2 \times 10^{18} \text{ cm}^{-3}$ .

at low doping concentrations is attributed to nonradiative transitions. The lifetime of the nonradiative channel is determined by the nonequilibrium minority carrier (hole) concentration and the concentration of traps participating in the recombination. In *n*-type semiconductors, the trap recombination rate is proportional to  $N_{TP}$  whereas the band-to-band recombination rate is proportional to  $np = N_D p$ . The ratio of radiative to nonradiative recombination rates is  $N_D/N_T$ . If  $N_T$  is independent of the doping concentration, radiative transitions increase with doping concentration. Thus, a higher efficiency is expected as  $N_D$  increases. This increase in efficiency is indeed observed experimentally.

The monotonic increase in luminescence efficiency with doping concentration also shows that luminescence killers (deep levels) do not increase with doping concentration. It has been shown in other material systems (e.g., Si in GaAs) that the luminescence efficiency *decreases* at the highest doping concentrations. The decrease has been attributed to compensating native defects.<sup>6</sup> However the results presented here show that in GaN the overall concentration of nonradiative defects does *not* strongly increase with doping concentrations.

In order to identify the physical nature of the near-band edge transition, different spectroscopic techniques were employed. Room temperature reflectance, transmittance, luminescence, and photoreflectance spectra of *n*-type GaN are shown in Fig. 4. Whereas reflectance, transmittance, and photoreflectance probe the absorption properties of semiconductors, luminescence probes the emission properties. Comparison of the luminescence peak energy with the band gap energy measured by the transmission, photoreflectance, and reflectance measurements reveals the absence of a Stokes shift, i.e., the luminescence peak occurs at the band-gap energy. The lack of a Stokes shift demonstrates that the dominant transition is due to band-to-band or excitonic recombination, i.e., it is *not* of *extrinsic* origin. The linewidth of the

near-band edge transition of the undoped sample is 47 meV which is in excellent agreement with the value of  $1.8kT = 45 \text{ meV}$  ( $T = 293 \text{ K}$ ) predicted for band-to-band electron-hole recombination. This agreement along with the lack of a Stokes shift between absorption and emission show that the near-band edge transition is consistent with band-to-band recombination.

In conclusion, the room temperature optical properties of GaN have been investigated for Si doping concentrations ranging from  $5 \times 10^{16}$  to  $7 \times 10^{18} \text{ cm}^{-3}$ . The luminescence intensity of the band-to-band transition increases monotonically with doping concentration, indicating the presence of luminescence killers in lightly doped GaN. The relevancy of the recombination centers is reduced at high doping concentrations. A comparison of the luminescence energy with the band-gap energy as measured by absorption and reflection spectroscopies shows that the near-band-gap transition is consistent with the band-to-band and excitonic recombination mechanism. The analysis of the transition linewidth in lightly doped GaN supports this conclusion. The luminescence linewidth increases from 47 to 77 meV as the doping concentration is increased from  $5 \times 10^{16}$  to  $7 \times 10^{18} \text{ cm}^{-3}$ . The broadening is consistent with the broadening predicted by a model which takes into account the concentration fluctuation of dopants.

<sup>1</sup>J. I. Pankove and J. A. Hutchby, *J. Appl. Phys.* **47**, 5387 (1976).

<sup>2</sup>T. Ogino and M. Aoki, *Jpn. J. Appl. Phys.* **19**, 2395 (1980).

<sup>3</sup>D. M. Hofmann, D. Kovaler, G. Steude, B. K. Meyer, A. Hoffmann, L. Eckey, R. Hertz, T. Detchprom, H. Amano, and I. Akasaki, *Phys. Rev. B* **52**, 16 702 (1995).

<sup>4</sup>D. H. Zhang, K. Radhakrishnan, and S. F. Yoon, *J. Cryst. Growth* **148**, 34 (1995).

<sup>5</sup>R. J. Malik, J. Nagle, M. Micovic, R. W. Ryan, T. D. Harris, M. Geva, L. C. Hopkins, J. Vandenberg, R. Hull, R. F. Kopf, Y. Anand, and W. D. Braddock, *J. Cryst. Growth* **127**, 686 (1993).

<sup>6</sup>L. Calderon, Y. Lu, H. Shen, J. Pamulapati, M. Dutta, W. H. Chang, L. W. Yang, and P. D. Wright, *Appl. Phys. Lett.* **60**, 1597 (1992).

<sup>7</sup>W. Shan, T. J. Schmidt, X. H. Yang, S. J. Hwang, J. J. Song, and B. Goldberg, *Appl. Phys. Lett.* **66**, 985 (1995).

<sup>8</sup>B. Monemar, *Phys. Rev. B* **10**, 676 (1974).

<sup>9</sup>M. Smith, G. D. Chen, J. Y. Lin, H. X. Jiang, M. Asif Khan, C. J. Sun, Q. Chen, and J. W. Yang, *J. Appl. Phys.* **79**, 7001 (1996).

<sup>10</sup>G. D. Chen, M. Smith, J. Y. Lin, H. X. Jiang, S.-H. Wei, M. Asif Khan, and C. J. Sun, *Appl. Phys. Lett.* **68**, 2784 (1996).

<sup>11</sup>J. Neugebauer and C. G. Van de Walle, *Appl. Phys. Lett.* **69**, 503 (1996).

<sup>12</sup>A. Hoffmann, L. Eckey, P. Maxim, J.-C. Holst, R. Heitz, D. M. Hofmann, D. Kovaler, G. Steude, D. Volm, B. K. Meyer, T. Detchprom, K. Hiramatsu, H. Amano, and I. Akasaki, *Solid-State Electron.* **41**, 275 (1997).

<sup>13</sup>W. Grieshaber, E. F. Schubert, I. D. Goepfert, R. F. Karlicek, Jr., M. J. Schurman, and C. Tran, *J. Appl. Phys.* **80**, 4615 (1996).

<sup>14</sup>For a large number of spheres, each defined by  $(N_A + N_D) (4/3) \pi r_s^3$ , the Poisson distribution approaches a Gaussian distribution. See, for instance, L. D. Landau and E. M. Lifshitz, *Statistical Physics* (Addison-Wesley, Reading, MA, 1970).

<sup>15</sup>For  $N_D < N_c$ , the Fermi level remains within the band gap. Thus broadening due to band filling does not occur in this doping range. In GaN, the effective density of states in the conduction band is  $N_c \approx 2.3 \times 10^{18} \text{ cm}^{-3}$ .

<sup>16</sup>E. O. Kane, *Phys. Rev.* **131**, 79 (1963).

<sup>17</sup>T. N. Morgan, *Phys. Rev.* **139**, A343 (1965).